Investigation into Multi-Phase Armature Windings for High-Temperature Superconducting Wind Turbine Generators

Liu, Dong; Song, Xiaowei; Deng, Fujin; Dong, Jianning

DOI
10.1109/TASC.2020.2967286

Publication date
2020

Document Version
Final published version

Published in
IEEE Transactions on Applied Superconductivity

Investigation Into Multi-Phase Armature Windings for High-Temperature Superconducting Wind Turbine Generators

Dong Liu, *Member, IEEE*, Xiaowei Song, *Member, IEEE*, Fujin Deng, *Senior Member, IEEE*, and Jianning Dong, *Member, IEEE*

***Abstract*—High-temperature superconducting (HTS) generators are being considered as a competitive candidate in large direct-drive (DD) wind turbines because of their features of being lightweight and compact. Normally a large air gap is inevitable in partially HTS generators, sacrificing the torque producing capability. In this paper, multi-phase armature windings for HTS generators are investigated to reduce the air gap length in HTS generators while not compromising generators' performance. Therefore, the torque density of HTS generators can be improved without any added costs. Five different multi-phase armature winding schemes are studied in the paper. Their performance regarding torque production and rotor losses in a 10 MW DD HTS generator are examined. The findings show that employing multi-phase armature windings can reduce the mechanical air gap without generating extra eddy current losses in the rotor, and the torque production can be improved by up to 9.1%. In addition, the alternating magnetic field reaching the HTS field winding are also reduced by using multi-phase armature windings, resulting in lower AC losses and cooling costs.**

***Index Terms*—AC loss, eddy current loss, multi-phase, HTS generator, torque, wind turbine.**

I. Introduction

HIGH temperature superconducting (HTS) generators are expected to be lightweight and compact compared to conventional synchronous generators. Thus, they are being considered in 10+ MW offshore direct-drive (DD) wind turbines to reduce the levelized cost of energy (LCOE) [1]–[6]. The state of the art of HTS generators for wind turbines is that within the EcoSwing project a full-scale 3 MW-class DD HTS generator has been successfully commissioned on a real wind turbine [7], [8].

Currently, feasible HTS generators are usually partially superconducting, i.e. only the field winding applies superconductors. As a result, the magnetic air gap in HTS generators is much larger than that in conventional generators [9]–[11]. There are two main reasons for this large magnetic air gap. One is that reasonable space is needed for a cryostat wall and thermal insulation required for operating the HTS field winding, which is very obvious. The other is that the mechanical air gap, i.e. the free space between the rotor and the stator, can not be as small as that in conventional machines. Otherwise, higher-than-accepted losses will be induced in the rotor, including eddy current losses in the electromagnetic (EM) shield and the cryostat wall [12], [13], and also AC losses in the HTS field winding [14].

However, the large air gap will sacrifice torque production of the HTS generator. As the torque density is one of the most critical factor to commercialize HTS generators in the wind industry, it is of great commercial interest to improve the torque density by reducing the air gap while not compromising the generator performance. From the vacuum and thermal insulation point of view, the space needed for the cryostat and thermal insulation materials, e.g. multilayer insulation (MLI), can hardly be reduced. Therefore, the only viable direction is trying to reduce the mechanical air gap while not bringing more rotor losses. Motivated by this thought, this paper evaluates the effects of employing multi-phase armature windings in HTS generators to reduce the mechanical air gap and to improve the torque production capability.

Multi-phase armature windings have been studied in the field of permanent magnet (PM) machines for better integration with power converters [15]–[21]. In the context of HTS generators, especially for the purpose of reducing the mechanical air gap, multi-phase armature windings have not been investigated yet. In a wind turbine's power conversion system using a DD HTS generator, multi-phase armature windings directly make use of currently equipped multiple power converters, as illustrated in Fig. 1. Hence, no additional costs will be added but only the winding connections should be adapted.

This paper investigates the effects of different multi-phase armature winding schemes on lifting the torque production of a 10 MW HTS generator by reducing the mechanical air gap while not increasing rotor losses. The minimum mechanical air gap and the best candidates among the studied multi-phase winding schemes will be identified. The findings show that employing

Manuscript received September 25, 2019; accepted January 9, 2020. Date of publication January 17, 2020; date of current version February 14, 2020. This work was supported in part by the Natural Science Foundation of Jiangsu Province of China under Grant BK20190486 and in part by the Fundamental Research Funds for the Central Universities under Grant 2018B02114. *(Corresponding author: Xiaowei Song.)*

D. Liu is with the College of Energy and Electrical Engineering, Hohai University, Nanjing CN-211100, China.

X. Song is with the Vestas Wind Systems A/S, Aarhus DK-8200, Denmark (e-mail: xiaowei.song0807@gmail.com).

F. Deng is with the School of Electrical Engineering, Southeast University, Nanjing CN-210096, China (e-mail: fdeng@seu.edu.cn).

J. Dong is with the Department of Electrical Sustainable Energy, Delft University of Technology, Delft NL-2628CD, Netherlands.

Color versions of one or more of the figures in this article are available online at https://ieeexplore.ieee.org.

Digital Object Identifier 10.1109/TASC.2020.2967286

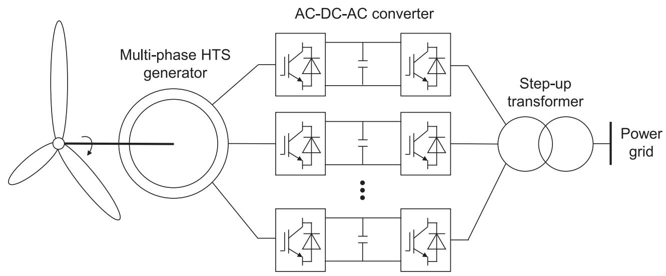

Fig. 1. Configuration of multi-phase armature windings connected to multiple power converters in a direct-drive wind turbine.

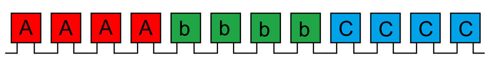

(a) $q = 4$, three phases

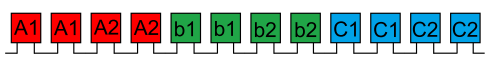

(b) $q = 4$, six phases (two sets of three phases)

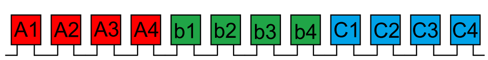

(c) $q = 4$, twelve phases (four sets of three phases)

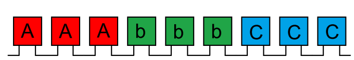

(d) $q = 3$, three phases

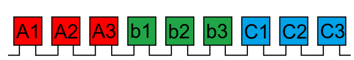

(e) $q = 3$, nine phases

Fig. 2. Winding distribution of multi-phase windings with the number of slots per pole per phase $q = 4$ and $q = 3$.

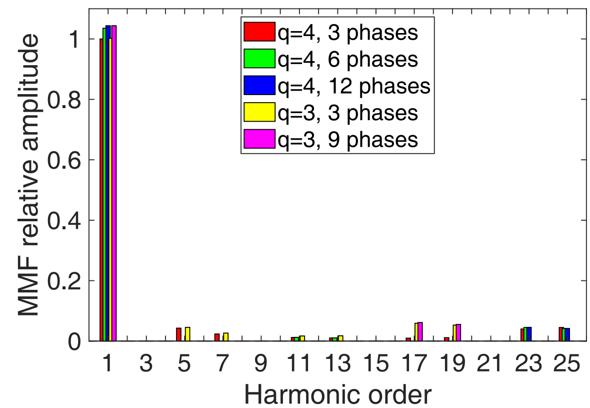

(a) MMF spectra of multi-phase windings

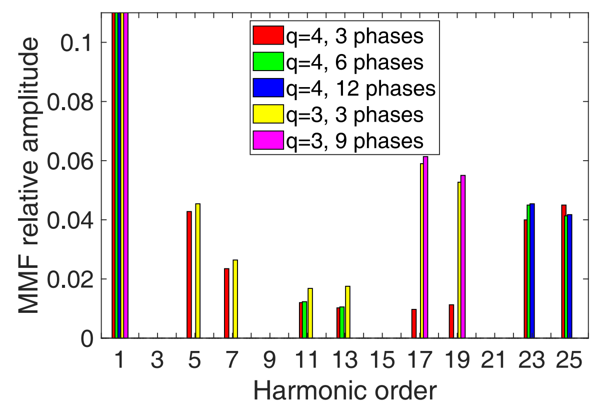

(b) Zoom-in at higher orders of MMF harmonics

Fig. 3. MMF spectra of the studied multi-phase windings.

multi-phase armature windings is a feasible and easy way to improve the torque density of HTS generators.

II. Concept of Multi-Phase Armature Windings

Multi-phase armature windings mean that the number of phases is larger than three [19], [22]. For integral-slot distributed windings, the number of phases is usually multiples of three but depends on the number of slots per pole per phase q. For example, nine phases consist of three sets of balanced three phases and q should be 3 or 6. Twelve phases consist of four sets of balanced three phases and q should be 4 or 8. Normally the value q is not very large, and thus 2, 3 and 4 are the most practical values. The winding distribution of six, nine, twelve phases, combined with the q value being 3 and 4, as sketched in Fig. 2, are studied in this paper. Single-layer windings are chosen for this investigation.

Magnetic field harmonics from the armature winding, other than the torque-producing harmonic, do not rotate synchronously with the rotor. The relative motion between these harmonics and the rotor induce losses in the HTS field winding and electrically conductive parts in the rotor, such as an EM shield made of copper.

To reduce harmonic contents in the magneto-motive force (MMF) of the winding, each set of three phases is shifted with the neighboring set by an angle in the phase current [15]. To maximize this effect, this angle should be $180^\circ/6 = 30^\circ$ for six phases, $180^\circ/9 = 20^\circ$ for nine phases, and $180^\circ/12 = 15^\circ$ for twelve phases. Combining such a shift in the phase current angle and also the space shift by a number of slots, certain MMF harmonics will be eliminated. As shown in Fig. 3(a), the multi-phase windings with the same number of q eliminate certain orders of harmonics. With $q = 4$, for example, six and twelve phases eliminate the 5th and 7th harmonics, whereas twelve phases eliminates the 11th and 13th harmonics. With $q = 3$, nine phases also eliminates the 5th, 7th, 11th and 13th harmonics. These harmonics are the primary contributors to induced losses in the rotor. However, some orders of harmonics are increased by applying the multi-phase windings, such as the 17th, 19th, 23 rd and 25th. Although these high orders of harmonics contribute to rotor losses, the contribution is much less compared to that from the lower orders.

Another notable advantage of multi-phase windings is that the fundamental component of MMF is slightly increased, as pointed out in Fig. 3(a). Apparently, a higher fundamental component of MMF helps to improve torque production.

Furthermore, it is common to employ multiple converters in wind turbines above 6 MW to share the high rated power [23]. Multiple phases directly make use of such currently applied multiple-converter configurations, thus there is no added cost in terms of power converters.

TABLE I
DESIGN PARAMETERS OF THE HTS GENERATOR

Air gap diameter	6112 mm
No. of pole pairs	24
No. of slots	576 for $q = 4$ 432 for $q = 3$
No. of turns per field pole	124
Stator slot height	160 mm
Stator slot width	13 mm
HTS field coil height	30.5 mm
HTS field coil Width	14 mm
Engineering current density in the field winding	120 A/mm^2
Armature current density	2.6 A/mm^2
Rated frequency	3.84 Hz

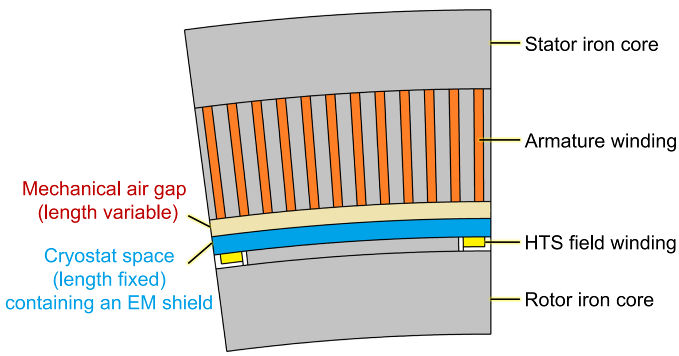

Fig. 4. Sketch of the HTS generator. One-pole model is shown, which forms a half symmetry for finite element analysis.

III. HTS GENERATOR DESIGN

The different multi-phase winding schems are compared under the same HTS generator. This HTS generator is designed for a 10-MW 9.6-rpm reference DD wind turbine [24]. The generator design is based on a prototype that has been experimentally proven in [25] but is optimized for the minimum levelized capital cost of energy for this wind turbine [26], [27]. Iron cores are used both in the rotor and in the stator to reach a low cost, and magnetic poles are chosen to be salient to balance the generator cost and the cryostat complexity. Table I list the key parameters of the designed HTS generator.

The superconducting field winding of this generator employs the second-generation (2-G) HTS wires (GdBCO) operating at 30 K. The cross-sectional dimension of the HTS field coils considers a fill factor of 0.7, accommodating 124 turns per pole. The engineering current density in the HTS field winding is 120 A/mm^2 to have a safety margin of 30% to the critical current density. Detailed design of the field winding duplicate that in our previous lab set-up, as reported in [28]. The cryostat and the EM shield are both cylindrical, and they enclose the whole HTS field winding and the rotor iron core, as depicted in Fig. 4.

The armature winding uses conventional copper conductors working at about 120 °C maintained by forced air cooling. The armature current density is set to 2.6 A/mm^2 to keep an affordable copper losses in the stator.

As indicated in Fig. 4, the magnetic air gap consists of two parts. One is for cryostat and MLI, which is nearly fixed because of the vacuum and the thermal insulation requirements. The other is the physical free space between the stator and the rotor, i.e. the mechanical air gap. The mechanical air gap length varies from 16 mm to 8 mm in this paper under different armature winding schemes. As 8 mm is approaching 0.1% of the air gap diameter, it is chosen to be the lower limit of the variation of mechanical air gap. It has been extensively recognized by electrical machine designers that it is a rule of thumb to use 0.1% of the air gap diameter as the air gap length of conventional machines. A mechanical air gap smaller than 0.1% of the air gap diameter is difficult to handle from the mechanical point of view.

IV. METHODOLOGY

The mechanical air gap of the HTS generator is the key variable in the study. With a specific winding scheme introduced in Section II, the torque production and the rotor losses are calculated and compared while varying the mechanical air gap from 16 mm to 8 mm. The total eddy current loss in the EM shield and the cryostat wall is chosen as the rotor loss. Because of EM shielding, AC losses in the HTS field winding are assumed to be negligible compared with eddy current losses in the EM shield and cryostat. Nevertheless, magnetic fields that reach the HTS field winding, which produce AC losses in the HTS field winding, will be briefly discussed.

The HTS generator with the original three-phase winding and the 16-mm mechanical air gap is selected as the baseline or reference case. Its torque production per unit length and its total eddy current loss are used as references to evaluate the performance of the multi-phase windings. Eddy current losses that are similar or lower than those in the reference case are desired.

The combinations of the mechanical air gap length and the multi-phase scheme, which result in the same or similar eddy current loss in the reference case, will be identified. Then, the torque production of the identified combinations will be compared with that of the reference case to see how much the torque can be increased. If the torque increase is significant, the mechanical air gap length and multi-phase winding scheme of the combination will be proposed to replace the original length (16 mm) and the original winding type (three-phase winding). Modelling, calculation and simulation with finite element methods (FEM) are used to obtain the torque, eddy current loss, flux density and other relevant quantities. The used FEM package is COMSOL Multiphysics.

V. EFFECTS ON TORQUE PRODUCTION

In this study, torque production per unit (axial) length is a function of the mechanical air gap and the type of the armature winding. The correlation is depicted in Fig. 5. The torque production with the 16-mm mechanical air gap, three phases ($q = 4$) is set to be the reference torque. The torques per unit length in other cases are normalized to this reference torque. As depicted in Fig. 5, with the same number of q, the multi-phase windings increase the torque. Note that the engineering current density in the field winding is fixed to 120 A/mm^2 for all the cases in Fig. 5 so that any differences in the torque production due to the field excitation are excluded.

Then, it is necessary to identify which mechanical air gap results in a similar eddy current loss as the reference case. As shown in Fig. 6, 9-mm mechanical air gap with six or twelve phases achieves this target for $q = 4$. For $q = 3$, the mechanical air gap between 12 mm and 11 mm achieves this target with nine phases.

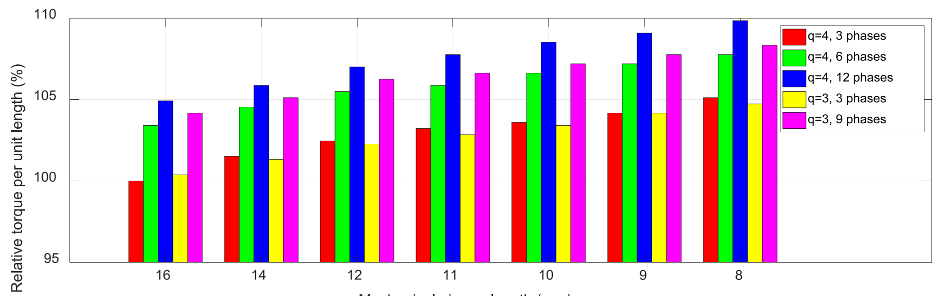

Fig. 5. Comparison of torque production.

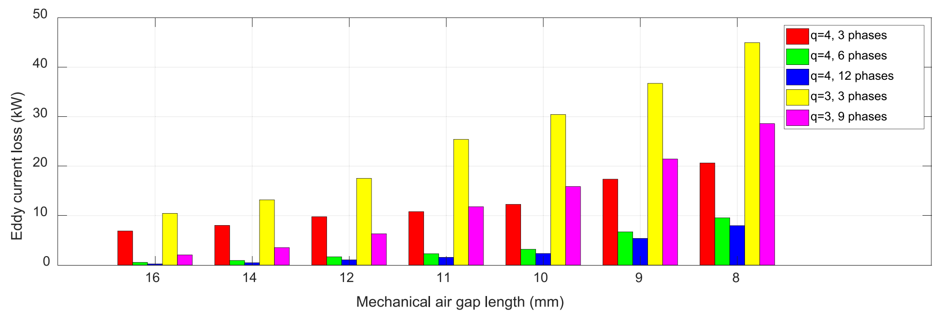

Fig. 6. Comparison of total eddy current losses.

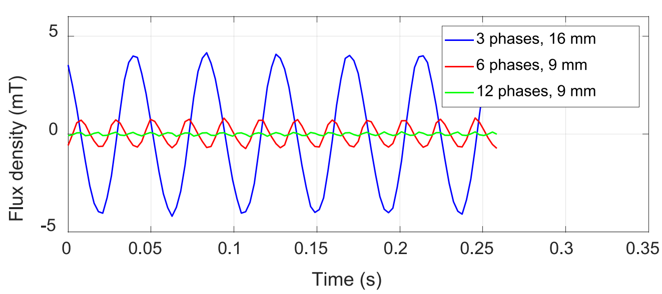

Fig. 7. Waveforms of radial flux density at one point of the HTS field winding. Three scenarios are compared.

Looking back at Fig. 5, for $q = 4$, the torque per unit length is increased by 7.2% with 9-mm gap and six phases, and 9.1% with 9-mm gap and twelve phases. For $q = 3$, the gap of 11 mm is the minimum and here the torque is increased by 6.2% with nine phases. As stated already, these torque enhancements are nearly free of charge since implementing multi-phases will not increase the cost.

The original mechanical air gap, i.e 16 mm, used for three-phase windings can be replaced by a much smaller gap, i.e. 9 mm, with six or twelve phase windings for $q = 4$. For $q = 3$, the gap can be shortened to 11 mm if a nine-phase winding is applied.

VI. Magnetic Fields on the HTS Field Winding

So far, only the eddy current losses in the EM shield and cryostat wall are considered as the rotor losses. As AC losses in the HTS field winding are related to thermal budgets of the cryogenic system, it is worth assessing the alternating magnetic fields on the HTS field winding because these fields are the main source of AC losses in the HTS field winding.

Fig. 7 plots the radial flux density (only the alternating component) at one point of the HTS field winding. Apparently, the two multi-phase windings for $q = 4$ effectively mitigate the amplitude of ripple fields at the minimum mechanical air gap obtained in Section V. The twelve-phase winding almost achieves a zero alternating field at the HTS field winding. Hence, one notable merit of multi-phase windings is smaller ripple magnetic fields on the HTS field winding, which directly reduces AC losses and benefits the cooling system design.

VII. Conclusion

It is inevitable to have a large magnetic air gap in currently feasible HTS generators that use a partially superconducting topology. Multi-phase armature windings can effectively reduce eddy current losses induced in the EM shield and the cryostat wall due to reduction of MMF harmonics. Therefore, the mechanical air gap can be reduced by applying multi-phase armature windings, which results in higher torque production while not compromising the generator performance. With a six-phase or twelve-phase winding, the mechanical air gap decreases from 16 mm to 9 mm, and the corresponding torque increase is 7.2% and 9.1% for $q = 4$. In the case of $q = 3$, the mechanical air gap can be reduced from 16 mm to 11 mm, and accordingly the torque rises by 6.2% with a nine-phase winding. Besides, the alternating magnetic fields that reach the HTS field winding are also minimized by employing a multi-phase armature winding, which helps to lower the cooling cost. Overall, the findings from the paper show that employing multi-phase armature windings is a promising and viable solution to improve the torque density of HTS generators.

REFERENCES

[1] K. S. Haran *et al.*, "High power density superconducting rotating machines development status and technology roadmap," *Supercond. Sci. Technol.*, vol. 30, 2017, Art. no. 123002.

[2] B. Maples, M. M. Hand, and W. D. Musial, "Comparative assessment of direct drive high temperature superconducting generators in multi-megawatt class wind turbines," Golden, CO, USA: National Renewable Energy Laboratory, 2010.

[3] A. B. Abrahamsen *et al.*, "Superconducting wind turbine generators," *Supercond. Sci. Technol.*, vol. 23, 2010, Art. no. 034019.

[4] B. B. Jensen, N. Mijatovic, and A. B. Abrahamsen, "Development of superconducting wind turbine generators," *J. Renewable Sustain. Energy*, vol. 5, 2013, Art. no. 023137.

[5] H. Polinder, J. A. Ferreira, B. B. Jensen, A. B. Abrahamsen, K. Atallah, and R. A. McMahon,"Trends in wind turbine generator systems," *IEEE J. Emerg. Sel. Top. Power Electron.*, vol. 1, no. 3, pp. 174–185, Sep. 2013.

[6] X. Li, S. Yu and Y. Wang, "A novel HTS claw-pole vernier machine using single excitation unit with stationary seal," *IEEE Trans. Appl. Supercond.*, vol. 29, no. 5, Aug. 2019, Art. no. 5201505.

[7] X. Song *et al.*, "Designing and basic experimental validation of the world's first MW-class direct-drive superconducting wind turbine generator," *IEEE Trans. Energy Convers.*, vol. 34, no. 4, pp. 2218–2225, Dec. 2019.

[8] A. Bergen *et al.*, "Design and in-field testing of world's first ReBCO rotor for a 3.6 MW wind generator," *Supercond. Sci. Technol.*, vol. 32, no. 12, Oct. 2019, Art. no. 125006.

[9] S. S. Kalsi, "Rotating AC machines," in *Applications of High Temperature Superconductors to Electric Power Equipment*, IEEE, 2011.

[10] R. Fair *et al.*, "Superconductivity for large scale wind turbines," U.S. DOE, Rep. DE-EE0005143, Apr. 2012. [Online]. Available: https://www.jlab.org/sites/default/files/magnet-group/other-published-papers/superconductivity_for_large_scale_wind_turbines.pdf

[11] R. Qu, Y. Liu and J. Wang, "Review of superconducting generator topologies for direct-drive wind turbines," *IEEE Trans. Appl. Supercond.*, vol. 23, no. 3, Jun. 2013, Art. no. 5201108.

[12] A. Jassal, H. Polinder and J. A. Ferreira, "Literature survey of eddy-current loss analysis in rotating electrical machines," *IET Electric Power Appl.*, vol. 6, no. 9, pp. 743–752, Nov. 2012.

[13] X. Sun *et al.*, "Core losses analysis of a novel 16/10 segmented rotor switched reluctance BSG motor for HEVs using nonlinear lumped parameter equivalent circuit model," *IEEE/ASME Trans. Mechatronics*, vol. 23, no. 2, pp. 747–757, Apr. 2018.

[14] Z. Xu and F. Grilli, "Modelling ac ripple currents in HTS coated conductors," *Supercond. Sci. Technol.*, vol. 28, no. 10, Apr. 2015, Art. no. 104002.

[15] J. Wang, R. Qu and Y. Liu, "Comparison study of superconducting generators with multiphase armature windings for large-scale direct-drive wind turbines," *IEEE Trans. Appl. Supercond.*, vol. 23, no. 3, Jun. 2013, Art. no. 5201005.

[16] Y. Demir and M. Aydin, "A novel dual three-phase permanent magnet synchronous motor with asymmetric stator winding," *IEEE Trans. Magn.*, vol. 52, no. 7, Jul. 2016, Art. no. 8105005.

[17] M. J. Duran *et al.*, "Six-phase PMSG wind energy conversion system base on medium voltage multilevel converter," in *Proc. Eur. Conf. Power Electron. Appl.*, Birmingham, U.K., 2011, pp. 26–33.

[18] H. S. Che *et al.*, "A six-phase wind energy induction generator system with series-connected DC-links," in *Proc. 3rd IEEE Int. Symp. Power Electron. Distrib. Gener. Syst.*, Aalborg, 2012, pp. 26–33.

[19] E. Levi, "Multiphase electric machines for variable-speed applications," *IEEE Ind. Electron.*, vol. 55, no. 5, pp. 1893–1909, May 2008.

[20] S. Brisset, D. Vizireanu and P. Brochet, "Design and optimization of a nine-phase axial-flux pm synchronous generator with concentrated winding for direct-drive wind turbine," *IEEE Trans. Ind. Appl.*, vol. 44, no. 3, pp. 707–715, May/Jun. 2008.

[21] Z. Shi *et al.*, "Torque analysis and dynamic performance improvement of a PMSM for EVs by skew angle optimation," *IEEE Trans. Appl. Supercond.*, vol. 29, no. 2, Mar. 2019, Art. no. 0600305.

[22] L. Parsa, "On advantages of multi-phase machines," *Proc. 31st Annu. Conf. IEEE Ind. Electron. Soc.*, Raleigh, NC, USA, 2005, pp. 1067–1071.

[23] Z. Chen *et al.*, Deliverable 3.31: Converter designs tailored to SC and PDD concepts, Tech. Rep. (INNWIND.EU). [Online]. Available: http://www.innwind.eu/publications/deliverable-reports

[24] P. Chaviaropoulos and A. Natarajan, "Deliverable D1.2.2: Definition of performance indicators (PIs) and target values," Oct. 2018. [Online]. Available: http://www.innwind.eu/publications/deliverable-reports/

[25] X. Song *et al.*, "Experimental validation of a full-size pole pair set-up of an MW-Class direct drive superconducting wind turbine generator," *IEEE Trans. Energy Convers.,* Early access, Dec. 9, 2019, doi: 10.1109/TEC.2019.2958613.

[26] D. Liu *et al.*, "Comparison of superconducting generator topologies for a 10 MW wind turbine applications," *Int. J. Appl. Electromag. Mech.*, vol. 53, no. S2, pp. S191–S202, 2017.

[27] D. Liu, H. Polinder, A. B. Abrahamsen and J. A. Ferreira, " Topology comparison of superconducting generators for 10-MW direct-drive wind turbines: cost of energy based," *IEEE Trans. Appl. Supercond.*, vol. 27, no. 4, Jun. 2017, Art. no. 5202007.

[28] X. Song *et al.*, "A full-size high-temperature superconducting coil employed in a wind turbine generator setup," *IEEE Trans. Appl. Supercond.*, vol. 27, no. 4, Jun. 2017, Art. no. 5201105.